The International Journal Research Publication's
ISSN:2251 1563
Research Journal of Science & IT Management

An Approach To Analyze Water And Ice For Multiradar Bands

Deepak Singh*, R.D. Garg, P.K Garg,
Department of Civil Engineering, IIT Roorkee, Roorkee - 247667, INDIA
Mobile: 91-8764131168, Email: deepakdotmail@rediffmail.com
***Keywords**: LPR, Greenland, Ganga*

Abstract

L and C Band radardata areavailable for studying terrestrial surfaces. Chandrayaan-1 had S band miniSAR and LRO is having X and S-Band miniRF radar sensors. Polarization products like Linear Polarization Ratio (LPR) and Circular Polarization ratio (CPR) derived from Stokes Parameters utilizes horizontally and vertically polarized received signals from the targets. LPR values for ice and water can be extracted from the terrestrial surface covering ice deposits over Greenland and water from fresh water lakes, rivers, oceans etc. These values are then interpolated for X and S bandswhich can be applied to terrestrial and extra-terrestrial surfaces for advanced studies.

1. Introduction:

Volume scattering increases with increase in grain size, internal layers and amount of snow. The size of ice crystal is 0.05-3.0 mm while the range of radar signal is in between 1 mm to 1 m(Dorothy, 1996; Polzar, 1993; Sorrentino, 2010). Radar waves in X, C, S, L and P bands penetrates through iceand are not scattered by relatively small ice crystals of snowpack (Matzler and Schanda, 1984; Ulaby and Stile, 1981;Waite and McDonald, 1970).Dry snowpack comprising of ice and snow layers results into enhanced backscatter as specular reflection (Matzler and Schanda, 1984). Older snow has large grain size than the newly formed snow which affects radar return. Individual grain size grows more than 3mm in diameter

Dielectric constant of snow is dependent on frequency of radar signal, wetness of snow, density of snow and temperature. At a lower temperature below 0° C, liquid water is present as a thin layer of film bound to crystals of ice(Hobbs, 1974). Below < 0 □ C temperatures, snow is assumed to be dry due to absence of water (Leconte et al, 1990). Snow is a mixture of ice and air, whose dielectric constants are 1.0 and 3.17 ± 0.07 for frequencies ranging between 1 MHz to microwave region (Evans, 1965). The DC of Snow is 1.2 to 2.0 when density of snow varies from 0.1 to 0.5g/cm^3 (Hallijkainen and Ulaby, 1986). DC of snow is also dependent on the presence of water in snow at a given radar band. Radar signal is absorbed by a thin layer of water present in the snow. Concentration of high proportion of water in dry snow enhances the dielectric constant of snow greater than 35 for frequencies below 20 GHZ or 15 m wavelength (Dorothy, 2006).

Received backscatter from the dry snow is sum of surface scattering at air/snow interface, volume scattering due to snow/soil interface and volume scattering from underground surface below snow. Radar scattering in dry snow, is dependent on depth and density of snow. Volume scattering in dry snow is due to the difference in the electrical properties of ice crystal and snow. Atmospheric scattering components is small and can be neglected (Bernier, 1987; Leconteetal, 1990;Ulaby and Stile, 1980).

Microwave wavelength bands X(2.5 cm to 3.75 cm), C(3.75 cm – 7.5 cm), S(7.5 cm – 15 cm), L(15 cm – 30 cm)(source: http://www.radioing.com/eengineer/bands.html) and P can penetrate into ground surface.Theoretical studies and experimental results indicate that, longer wavelength can penetrate deeper into dry soil.L band can penetrate into alluvial soils, sandy dry soils and pure ice, whereas C-band is suitable for surface related studies (Lillesand et al, 2008). Penetration depth of SAR microwave is a function of soil moisture(Matt and Deniss, 2003) which points towards signal penetration up to 500 mm.Penetration depth is given by the relation, $d = 9.2^* \lambda$(Elachi, 1988), where λ is the wavelength.Putting the values of λ for X, C, S, L and P bands, the penetration depths are obtained as 23.0-34.5 cm, 34.5-69 cm, 69-138 cm, 138-276 cm, 276-920 cm respectively. Microwave signal of 1.3 GHz may penetrate between the range of 1 m to 4 m under dry soil conditions (Long, 1975).Latest development of technologies in remote sensing, computing, sensors, image processing,

and microwave technologies have made it possible to analyze features under wet and dry conditions (Henderson, 1998).

Images obtained from like polarized images would be different from those obtained from cross polarized due to the difference in physical processes involved in the two types of returns (Fung and Ulaby, 1985).Additional information is gathered from this relative difference in values, and provides a clue for interpreting target surfaces.Lewis (1968, 1969)studied polarization with respect to features with ka, HH, HV, VV and VH, polarized images, where HV was found to be good for obtaining signals from rural building and farmsteads followed by HH, VH and VV in the importance of order. Cross polarization enhances large shopping centers, institutional complexes, and Industrial areas which lacks natural vegetation. Central Business Districts, bridges are observable with HH polarization to interpret urban land use. Bryan (1975) used multi frequency and multipolarizationimages for interpretation of urban features.Henderson and Mogilisky (1987) study indicated that of the seven land use categories, only commercial category produced a significant difference in radar signal response between HH and HV polarization.

Information content in an image can be represented, mathematically in terms of four stokes parameters S_1, S_2, S_3 and S_4(Stokes, 1852, Raney 212) and are defined as, $S_1 = |E_H|^2 + |E_V|^2$, $S_2 = |E_H|^2 - |E_V|^2$, $S_3 = 2\,Re\langle E_H E_V^*\rangle$ and $S_4 = -2Im\langle E_H E_V^*\rangle$. First stokes parameter represents, total power (or total intensity) of received, polarized, horizontal and vertical components of electromagnetic field (EM) and is the sum of horizontal and vertical components. Second stokes parameter is the difference between the two polarized components. Third stokes parameter is the cosine of the average phase between the two components and the fourth stokes parameter is sine of the average phase between the two components (Reid, 2010). It can be represented in terms of co-polarized HH (horizontal transmit and horizontal receive) and cross-polarized HV (horizontal transmit and vertical receive) bands of ALOS Advanced Land Observing Satellite) PALSAR (Phased Array type L-band Synthetic Aperture Radar), where Band1 is the horizontal portion of received EM field (i.e. HH), Band 2 is thevertical portion of received EM field (i.e. HV) and □ is the phase difference between HH and HV. This can be represented in terms of bands of microwave radar data as S1= Band1 + Band2, S2= Band + Band2, S3 = 2*Band1$^{1/2}$ * Band2$^{1/2}$* cos □ and S4 = □ 2 * Band1$^{1/2}$ * Band2$^{1/2}$ * $sin\ \delta$.

Polarization products like Circular Polarization Ratio (CPR) derived from Same Sense Circular Polarization (SC) and Opposite Sense Circular polarization, Degree of Polarization (m)(Reid, 2010), Linear Polarization Ratio (LPR) etc. are calculated as SC = 0.5*$S1$ – 0.5*$S4$, OC= 0.5*$S1$ + 0.5*$S4$, $CPR = SC / OC$, $m = (S_2^{\,2} + S_3^{\,2} + S_4^{\,2})^{1/2} / S_1$, $LPR = (S_1 + S_2) / (S_1$ □ $S_2)$. CPR is extensively used for study of planetary ice(Spudis, 2010).

2. Study Area and Datasets

Four separate locations over Greenland and four distinctsites along the path of river Ganga are selected for derivation of LPR and CPR values from L band ALOS PALSAR (AP) and C BandSentineldatasets, downloaded from Alaska satellite facility (ASF). The details of ice datasets from four distinct locations of Greenland and water datasets from river Ganga at four distinct locationsin L Band viz. Rishikesh, Haridwar, Kanpur and Varanasi are detailed in Table 1.C Band datasets from Greenland and water samples sites along the path of river Ganga are tabulated in Table 2. The study sites form Greenland and river Ganga from C and L band are depicted in Figure 1.

Table 1:L Band datasets from Greenland and river Ganga

S.No.	Locations	Datasets	Date/Time	Latitude/Longitude
1.	Greenland 1	ALPSRP080221600	28/07/2007; 00:31:36	79º 23' N, 50º 55' W
2.	Greenland 2	ALPSRP080221590	28/07/2007; 00:31:28	78º 55' N, 50º 11' W
3.	Greenland 3	ALPSRP081971600	09/08/2007; 00:27:17	79º 22' N, 50º 06' W
4.	Greenland 4	ALPSRP078761610	18/07/2007; 00:18:53	79º 49' N, 48º 57' W
5.	Ganga - Rishikesh	ALPSRP083970590	22/08/2007; 17:17:05	30 □ 06′ N, 78 □ 18′ E
6.	Ganga - Haridwar	ALPSRP079740580	24/07/2007; 17:19:10	29 □ 57′ N, 78 □ 11′ E
7.	Ganga- Kanpur	ALPSRP085720510	03/09/2007; 17:11:39	26 □ 28′ N, 80 □ 21′ E
8.	Ganga- Varanasi	ALPSRP086740490	10/09/2007; 17:00:36	25 □ 19′ N, 83 □ 02′ E

Table 2: C-Band Sentinel datasets fromGreenland and river Ganga

S.No.	Locations	Datasets	Date/Time
1.	Greenland	S1A_EW_GRDM_1SDH_20150302	02/03/2015; 11:19:01
2.	Ganga- Rishikesh	S1A_IW_GRDH_1SDV_20150303	03/03.2015;00:42:56
3.	Ganga- Haridwar	S1A_IW_GRDH_1SDV_20150303	03/03.2015;00:42:56
4.	Ganga- Kanpur	S1A_IW_GRDH_1SDV_20150226	26/02/2015; 00:35:53
5.	Ganga- Varanasi	S1A_IW_GRDH_1SDV_20160223	23/02/2016;00:19:47

3. Methodology:

The proposed methodology to study ice and water over the terrestrial surface from L-Band AP and C-Band Sentinel is shown in Figure 2. Datasets of ice from Greenland and water from river Ganga is obtained from C-Band Sentinel as well as well as from L-Band AP. Distinct locations are identified over Greenland and River Ganga. As the distribution of ice is uniform over Greenland surface, the sites are randomly selected. The sites for water are selected from the river Ganga across its stretch atRishikesh, Haridwar, Kanpur and Varanasi. The images are accessed and processed in ENVI software. The images in Sentinel C-Band are flipped left to right in ENVI for obtaining the correct images. Stokes parameters are derived from HH and HV received signals. The LPR values are calculated from Stokes parameters and applied to the images. The LPR values are obtained for fresh craters, water, ice and rough surface. The calculated values in C and L-Band data are interpolated for X and C bands to be applied over terrestrial and planetary surface for identification of pixels for water, ice and fresh craters.

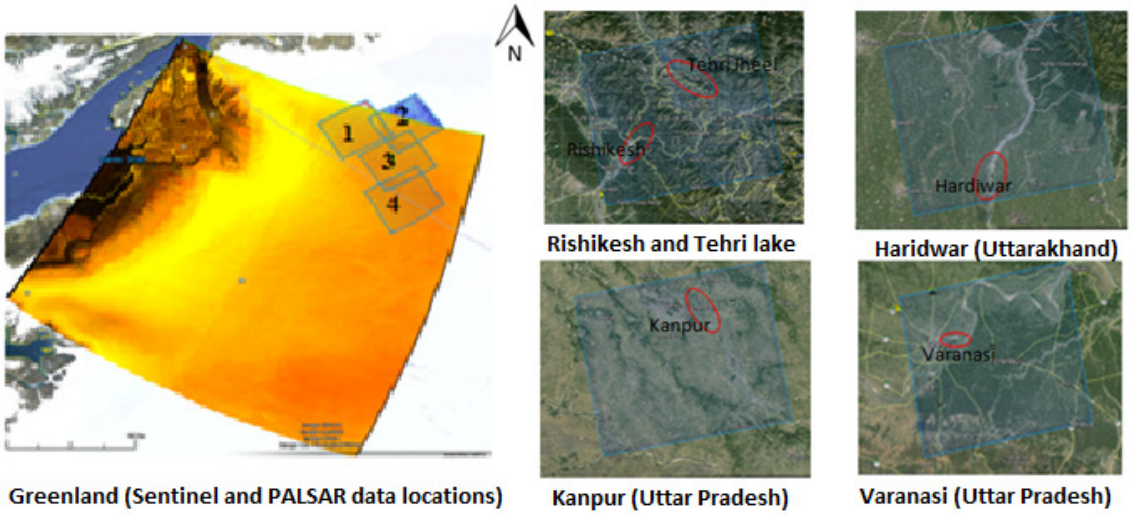

Figure 1: Study sites of ice and water samples

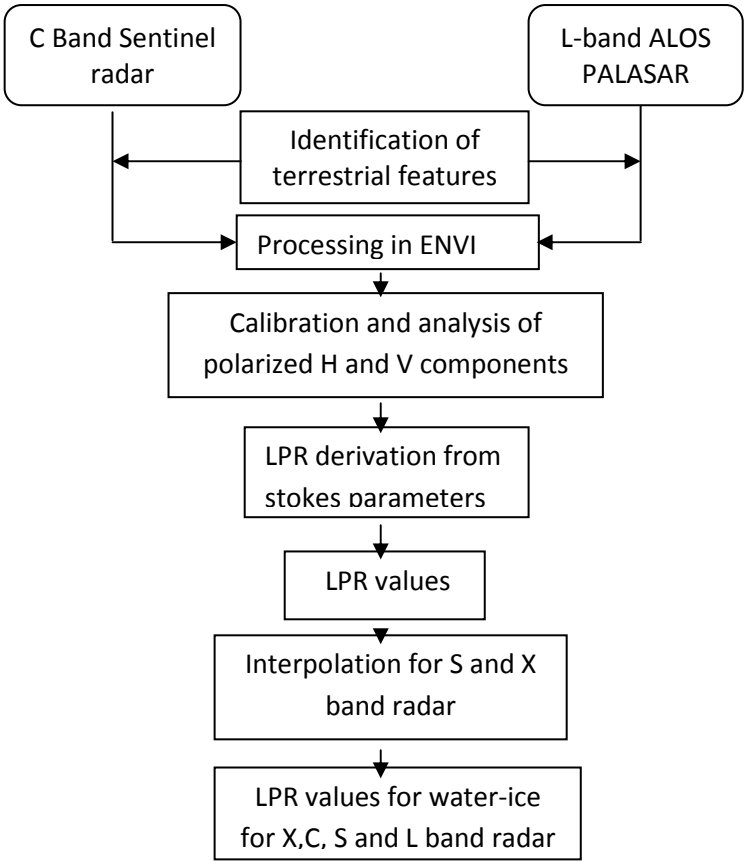

Figure 2:Flowchart of the Proposed Methodology

4. Results And Discussions:

The mean linear polarization ratio(LPR) value of20,000ice pixels are calculated from four distinct locations of Greenland, using C-Band Sentinel and L-Band APdata. The values obtained are 2.23 and 4.69 respectively as tabulated in Table 3.

Table3: LPR values from four distinct locations of Greenland in C and L Band

C-Band data		
Greenland	No. of Pixels	LPR Mean
Site 1	5000	2.14
Site 2	5000	2.17
Site 3	5000	2.26
Site 4	5000	2.35
Total Pixels = 20,000		Overall Mean = 2.23

L-Band data		
Greenland	No. of Pixels	Mean
Site 1	5000	4.27
Site 2	5000	4.62
Site 3	5000	4.75
Site 4	5000	5.11
Total Pixels = 20,000		Overall Mean = 4.69

Similarly, LPR values of water from river Ganga using C-Band Sentineland L band AP data, shows variations at four distinct locations at Rishikesh, Haridwar, Kanpur and Varanasi.In the combined results of figure 3, it is observed that the behavior of C-Band radar signal is comparatively similar at all the four separatelocations. The mean value of LPR is 0.58 with minimum value of 0.53 at Kanpur and maximum value of 0.63 at Rishikesh.

The International Journal Research Publication's
ISSN:2251 1563
Research Journal of Science & IT Management

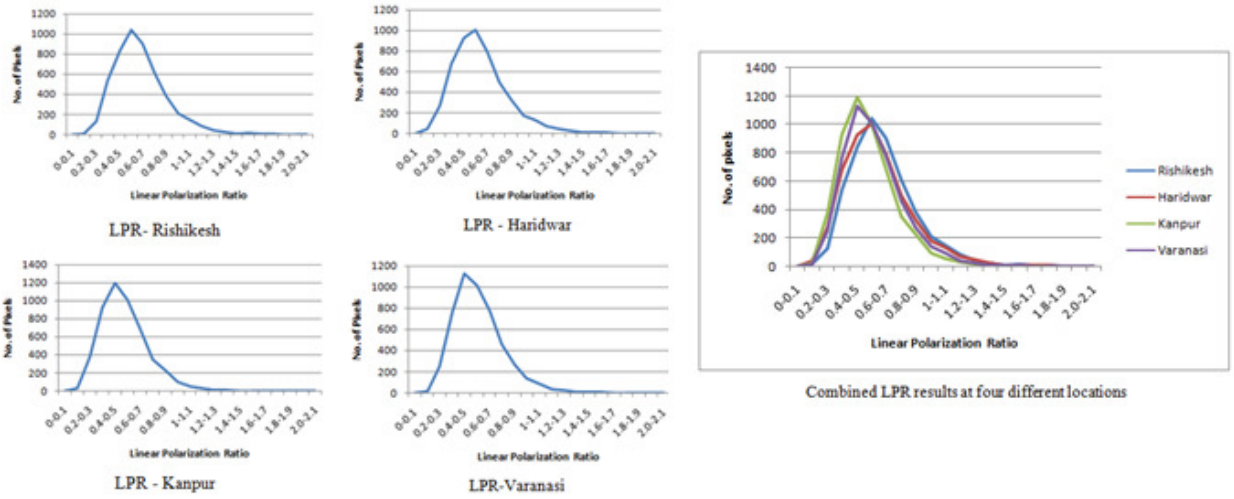

Figure 3: LPR variations at four distinct locations of River Ganga

The LPR variations over Greenland and river Ganga shows two distinct distribution curves corresponding to ice and water indicated in Figure 4. Distribution curves of ice are similar at distinct locations over Greenland. Similarly, Water distribution curves are similar at all the selected locations along the river path. This makes it is possible to separate the range of LPR values between ice and water.

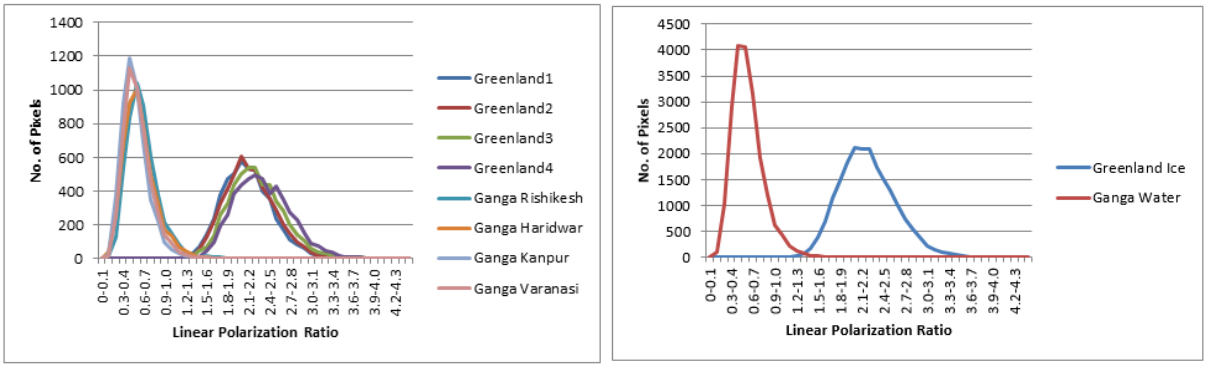

Figure 4: LPR values for water and icein C-Band Sentinel sensors.

Figure 4 shows, variations in LPR values for water and ice, the mean of both the curvesarewidelyseparated. As there is no overlapping of pixels, the range of LPR values can be directly utilized in the applications using C-Band sensors on terrestrial and extra-terrestrial surfaces like Moon, Mars, asteroids,etc. The combined results for ice and water using C Band Sentinel radar sensor is also depicted in Figure 4. The distribution curves for ice and water are distinctly separate, which can be used to utilize the range of LPR values individually for ice and water.A substantial gap exists between water and ice distribution curves in Sentinel C-Band radar. However, in L-Band AP, the gap is reduced. It can be inferred that with P band microwave sensor, the gap between water and ice would further be reduced, allowing the derivation of maximum informational content from water bodies.

LPR values of water from river Ganga at Rishikesh in C-Band Sentinel radar is shown in Table 4. A total of 5000 pixels are selected from various sites of Rishikesh, Haridwar, Kanpur and Varanasi along the path of river Ganga, after visualizing the images having sufficient water quantity.

The weighted mean of LPR values of 5000 pixels of Rishikesh is calculated as,

$$\text{Weighted mean} = \bar{x} = \frac{\sum_{i=1}^{n}(x_i * w_i)}{\sum_{i=1}^{n} w_i} = \frac{0.67*209+0.65*1216+\cdots\ldots\ldots\ldots\ldots+0.49*105+0.51*66}{5000} = 0.63$$

The weighted mean of LPR values of water from river Ganga at Rishikesh is obtained to be 0.63, which is much lower than that obtained using L-Band AP.The weighted LPR mean of 5000 water pixels from river Ganga at Haridwar is0.59, at Kanpur is 0.53 and at Varanasi is 0.56.Hence the average value of all the four stations is: (0.63+0.59+0.53+0.56)/4 ~0.58. It is observed that the calculated LPR values ofwater from river Ganga using C-Band Sentinel datasets is lower than that using L-BandAP datasets from similar locations.

LPR values are also obtained using L-Band ALOS PALSAR datasets. The LPR values of 10,000 pixels of water from river Ganga from Tehri lake is 2.77 as shown in Table 4, which is the purest water of all the locations under study.The LPR value of 10,000 water pixels from river Ganga at Haridwar is 2.01, at Kanpur is 2.58 and at Varanasi is 2.54.Mean of all the four stations viz. Rishikesh, Haridwar, Kanpur and Varanasi is:(2.77+2.005+2.58+2.5355)/4=2.47.

Table 4: LPR values of water from river Ganga in C Band Sentinel and L Band PALSAR

LPR of water in C Band		
Sites	No. of Pixels	Mean LPR
Rishikesh	5000	0.63
Haridwar	5000	0.59
Kanpur	5000	0.53
Varanasi	5000	0.56
Overall Mean LPR = 0.58		

LPR of water in L Band		
Sites	Total Pixels	Mean LPR
Tehri Lake	10,000	2.77
Haridwar	10,000	2.01
Kanpur	10,000	2.58
Varanasi	10,000	2.54
Overall Mean LPR = 2.47		

LPR values of water and ice in C-Band varies significantly from LPR values in L-Band. The distribution curves in C and L bands are distinct, which allows to find out the interpolated values for X and S band. X, C, S, L and P Band varies in ascending order of wavelength in EM spectrum of microwave region. The significant gap in ice and water distribution curves allows toseparate the ranges of water and ice. Variations in LPR in C band for water and ice narrows down in L band, as is evident in Figure 5.

4.1Derivation of unique LPR range of values for water and ice using L-Band ALOSPALSAR

Distributions curves for Greenland are constructed from four datasets covering north-western region of Greenland. The mean LPR value of ice is 4.69, which is observed to be much higher than the LPR of other features like craters and water, but lesser than urban settlements and rough surfaces. The Greenland is covered with melted water over the surface during the summer months of July, which is reflected in the lowering of LPR values for datasets 1, 2 and 4. Presence of water decreases the LPR values. Distribution curves based on LPR values of water in L-Band, drawn from, four segments of river Ganga at Rishikesh, Haridwar, Kanpur and Varanasi as shown in Figure 7.

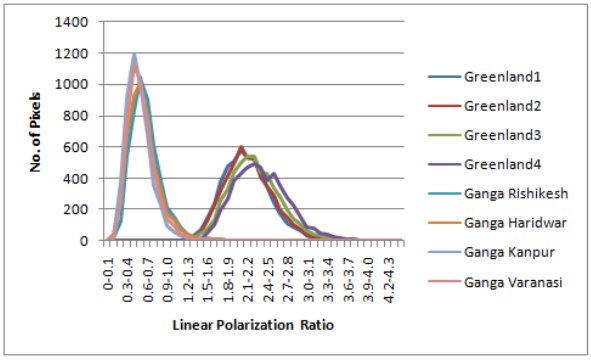

LPR for water and ice in C band

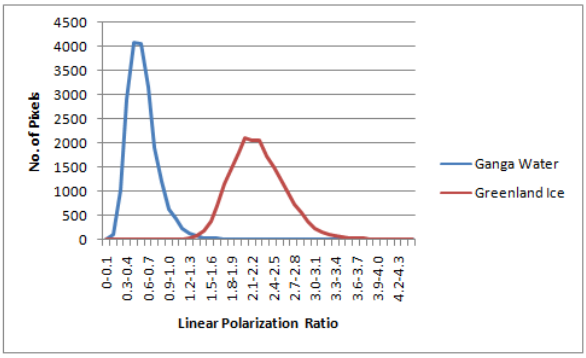

CombinedLPR for water and ice in C band

The International Journal Research Publication's
ISSN:2251 1563
Research Journal of Science & IT Management

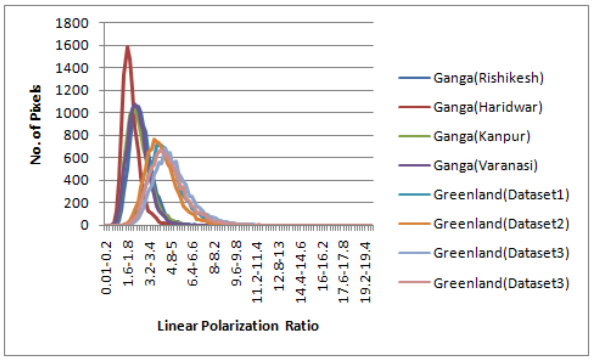

LPR for water and ice inL Band

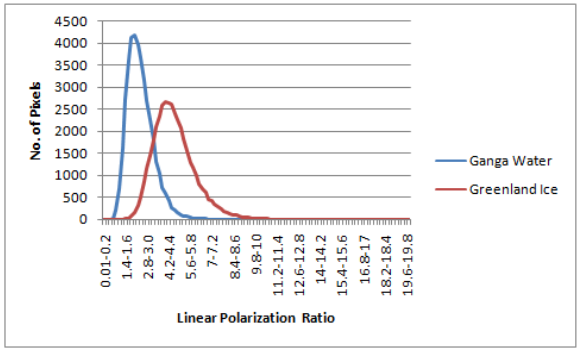

Combined LPR for water and iceinL Band

Figure 5: Linear Polarization ratio for water and ice in C and L band.

The mean LPR value of intersection of water distribution curve of River Ganga at Rishikesh with ice distribution curves is 3.7. Similarly, the mean LPR value of intersection of water distribution curve from River Ganga at Haridwaris 2.95, at Kanpur is 3.5, at Varanasi is 3.45.

Hence taking the average of all the four intersection points, we get a mean value of intersection as = (3.7+2.95+3.3+3.45)/4= 3.35
Mean LPR value of Greenland ice (4 locations) = 4.69
Mean LPR value of Ganga river (at 4 locations) = 2.49

For water range,

Higher value = 3.35= 2.49 + $\frac{2.49*x}{100}$

or$x$ = (335-249)/2.49 = 34.54%

hence, *lower value* = 2.49 - $\frac{2.49*x}{100}$

= 2.49 – (2.49 * 34.54)/100

= 1.63

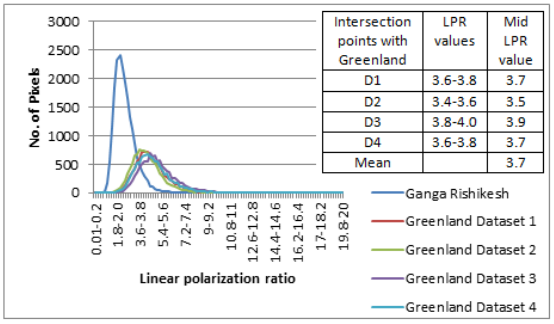

Intersection points with Greenland	LPR values	Mid LPR value
D1	3.6-3.8	3.7
D2	3.4-3.6	3.5
D3	3.8-4.0	3.9
D4	3.6-3.8	3.7
Mean		3.7

Ganga (Rishikesh) water and Greenland Ice

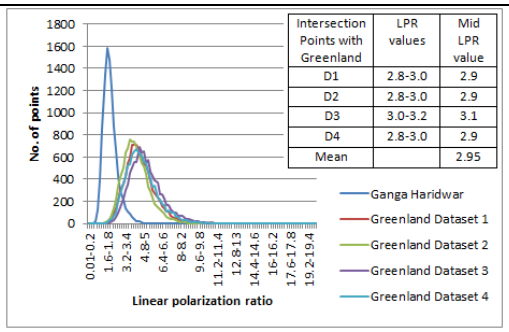

Intersection Points with Greenland	LPR values	Mid LPR value
D1	2.8-3.0	2.9
D2	2.8-3.0	2.9
D3	3.0-3.2	3.1
D4	2.8-3.0	2.9
Mean		2.95

Ganga (Haridwar) water and Greenland Ice

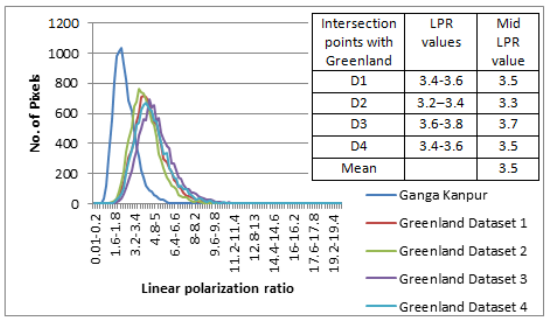

Intersection points with Greenland	LPR values	Mid LPR value
D1	3.4-3.6	3.5
D2	3.2–3.4	3.3
D3	3.6-3.8	3.7
D4	3.4-3.6	3.5
Mean		3.5

Ganga (Kanpur) water and Greenland Ice

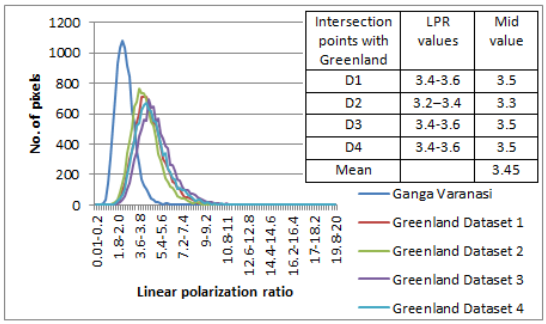

Intersection points with Greenland	LPR values	Mid value
D1	3.4-3.6	3.5
D2	3.2–3.4	3.3
D3	3.4-3.6	3.5
D4	3.4-3.6	3.5
Mean		3.45

Ganga (Varanasi) water and Greenland Ice

D1-Dataset1, D2-Dataset 2, D3-Dataset 3, D4-Dataset 4

Figure 7: Distribution curves of Ganga river water and Greenland Ice (10,000 pixels)

For ice range,

Lower value = 3.35= 4.69 - $\frac{4.69*x}{100}$

Or x = (469-335)/4.69 = 28.57

Hence, *higher value* = 4.69 + $\frac{4.69*\square}{100}$

= 4.69 + (4.69 * 28.57)/100 = 6.03

Hence, the upper range of value for ice is 6.03. The values lower than 1.63 can be assigned to craters and volcanoes, as is observed in their independent studies. LPR values greater than 6.03 are observed from rough surfaces and urbanized areas.The range of values derived for ice, water and craters,are finally tabulated in Table 5.

Table 5: Final estimates of LPR ranges in L band sensor for terrestrial surface

S.No.	Features	LPR values
1	Crater/Volcano	0.1-1.63
2.	Water	1.63- 3.35
3.	Ice	3.35- 6.03

Table 6: LPR values ranges for X and S, derived from C and L bands

Microwave Bands	Crater	Water	Ice	Rough
X	0.1-0.12	0.12-0.46 (mean - 0.25)	1.21-2.56 (mean- 1.80)	2.56 – max. value
C	0.1-0.15	0.15-1.25 (mean- 0.58)	1.25-3.452.23 (Mean- 2.95)	3.45-max value
S	0.1-0.19	0.19-2.56 (mean-1.14)	1.21-2.56	2.56- max value
L	0.1-0.3	0.3-5.7 (mean-2.47)	1.5-8.5 (mean-4.69)	8.5-max value

The interpolated values for X and S radar bands are indicated in Table 6. The variations of LPR with multiple radar bands are depicted in Figure 8. The results can be directly implemented further over other terrestrial features and extra-terrestrial surface like Moon, Mars, asteroids etc. for search of water-ice

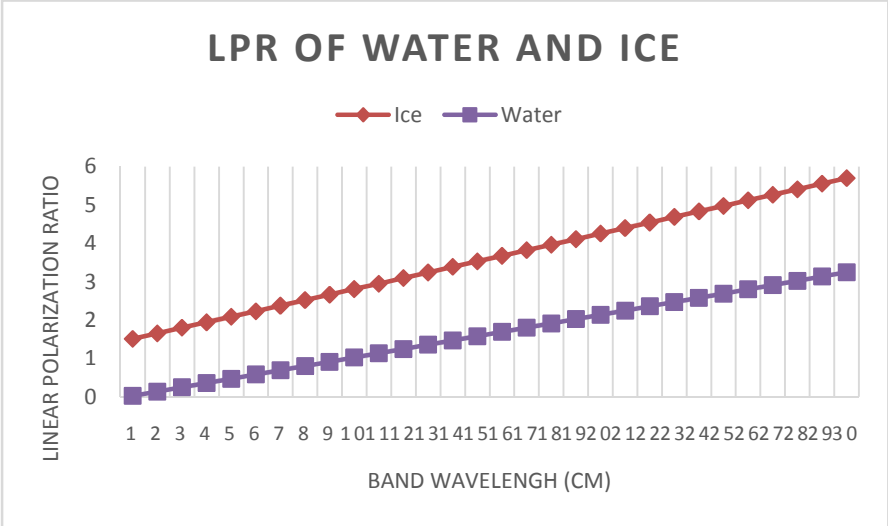

Figure 8: LPR variations of water and Ice in four different Bands

5. Conclusions:

Most of the radar sensors data, freely available from different agencies on terrestrial surface, is in L and C band, while the radars sensors operating on planetary surfaces are S and X band. Chandrayaan-1 and LRO utilized X and S band miniSAR and miniRF radar sensors. LPR and CPR values for water and ice were obtained using L band ALOS PALSAR and C Band Sentinel data from separate locations of Greenland and Ganga river. The values of water from river Ganga from various locationsand values of ice from Greenland formed similar distribution curvesfor water and ice respectively. These two classes were widely separated in C band and L band data. These values were then interpolated for X and S bands radar sensors, which can be applied to water-iced studies related to extra-terrestrial surfaces utilizing S and X band sensors.

References:

1. Bernier, P.Y.(1987), Microwave Remote Sensing of Snowpack Properties: Potential and Limitations, Nordic Hydrology, Vol. 18, pp. 1-20.
2. Bryan, M.L.(1975), Interpretation of an Urban Scene Using Multi-Channel Radar Imagery, Remote Sensing of Environment, Vol. 4, No.1, p.49-66.
3. Dorothy K. Hall, (1996), Remote sensing applications to hydrology; imaging radar Hydrological Sciences Journal, 4, Vol, 41.
4. Dorothy K. Hall, (2006), Estimation of Snow Extent and Snow Properties, Encyclopedia of Hydrological Sciences.
5. eEngineer – Radio Frequency Band Designations". http://www.radioing.com/eengineer/bands.html (retrieved 2011-11-08).
6. Elachi, Charles, (1988), Spaceborne Radar Remote Sensing: Applications and Techniques, IEEE press, New York, pp. 11-20.
7. Evans, S.(1965),The Dielectric Properties of Ice and snow- A review. Journal of Glaciology,Vol. 5, pp. 773-792.
8. Fung, Adrain K. andUlaby, F.T. (1983), Matter Energy Interaction in the Microwave Region, Manual of Remote Sensing, Vol. 1, Second Edition, Chapter 4, pp.115-117.
9. Hallikainen, M. and Ulaby, F.T. (1986), Dielectric and Scattering Behavior of snow at Microwave frequencies, Proceedings of the international Geoscience and remote sensing Symposium, 8-11 September, Zurich, Switzerland, pp. 87-91.
10. Henderson, F.M. and Mogilski, K.A. (1987), Urban Land Use Separability as a Function of Radar Polarization, International Journal of remote Sensing, Vol. 8, No.3, p. 441-448.
11. Henderson, F.M. and Lewis, A.J. (1998), Principles& Applications of Imaging Radar, 3Ed., Manual of Remote Sensing, John Wiley and Sons,
12. Hobbs, P.V. (1974), Ice Physics, Clarendon Press, Oxford, pp. 837.
13. Leconte, R.and Pultz, T. (1990), Utilization of SAR data in the monitoring of snowpacks and wetlands. Proceedings of the workshop on Applications of Remote Sensing in Hydrology, 13-14 February, Saskatoon, Saskatchewan, pp. 233-258.
14. Lewis, A.J. (1968), Evaluation of Multiple-Polarized Radar Imagery for the Detection of Selected Cultural Features, NASA Technical Letter, NASA 130, Reprinted in Holtz, R. (Editor), 1973), The Survellant Science, Houghton Mifflin, Boston, p.297-313.
15. Lewis, A.J. (1969), Detection of Linear Cultural Features with Multipolarized Radar Imagery, Proceedings of the Sixth International Symposium on Remote Sensing of Environment, University of Michigan, Ann Arbor, MI, pp. 879-893.
16. Lillesand, T.M., Kiefer, R.W. and Chipman, J.W. (2008). Remote sensing and Image Interpretation, 6thEd., John Wiley and Sons.
17. Long, M.W. (1975), Radar Reflectivity of Land and Sea, D.C. Heath & Co.., Lexington, MA, 366p
18. Matzler, C. and Schanda, E. (1984), Snow Mapping with Active Microwave Sensors, International Journal of Remote Sensing, Vol. 5, No. 2, pp. 409-422.

19. Raney, R.K., Cahill, J.T.S., Patterson, G.W., Bussey, D.B.J. (2012),The m-chi decomposition of hybrid dual-polarimetric radar data with application to lunar craters, Journal of Geophysical Research,117, 1-8.
20. Reid M. et al., PDS data product software interface specification, mini-RF advanced technologies, Lunar Reconnaissance Orbiter (LRO) Payload Operations Center, 2010.
21. Sorrentino, R. and Bianchi, Giovanni (2010) Microwave and RF Engineering, John Wiley & Sons, p. 4.
22. Spudis, P. D., Bussey, D.B.J., Butler, B., Carter, L., Chakraborty, M., Gillis Davis, J., Goswami, J., Heggy, E., Kirk, R., Neish, C., Nozette, S., Patterson, W., Robinson, M., Raney, R. K., Thompson, T., Thomson, B.J. and Ustinov, E. (2010), Results of the Mini-SAR imaging radar, Chandrayaan-1 mission to the Moon", 41st Lunar and Planetary Science Conference, The Woodlands Texas (1533): p. 1224.
23. Stokes, G. G. (1852), On the composition and resolution of streams of polarized light from different sources,Trans. Cambridge Philos. Soc., **9**, 399–416.
24. Nolan, M. and Dennis, R.F. (2003), Penetration Depth as a DInSAR Observable and Proxy for Soil Moisture,IEEE transactions on Geosciences and Remote Sensing, 41, 532-537.
25. Pozar, David M. (1993). Microwave Engineering Addison–Wesley Publishing Company. ISBN 0-201-50418-9.
26. Ulaby, F.T. and Stiles,W.H. (1980),The Active and Passive Microwave Response to Snow Parameters 2. Water Equivalent of dry snow, Journal of Geophysical Research, 85(C2):1045-1049.
27. Ulaby, F.T. and Stiles,W.H. (1981), Microwave Response of Snow, Advanced Space Research, 1:131-149.
28. Waite, W.P, and MacDonald, H.C. (1970), Snow field Mapping with K-band Radar, Remote Sensing of Environment,Vol. 1, pp.143-150.